

## Micromechanical Properties of Gd<sub>3</sub>Ga<sub>5</sub>O<sub>12</sub> Crystals Irradiated with Swift Heavy Ions

G.M. Aralbayeva<sup>1</sup>, I. Manika<sup>2</sup>, Zh. Karipbayev<sup>1</sup>, Y. Suchikova<sup>3,\*</sup>, S. Kovachov<sup>3</sup>, D. Sugak<sup>4</sup>, A.I. Popov<sup>2</sup>

<sup>1</sup> Faculty of Physics and Technical Sciences, L.N. Gumilyov Eurasian National University, 010008 Astana, Kazakhstan

<sup>2</sup> Institute of Solid State Physics, University of Latvia, 8, Kengaraga, LV-1063 Riga, Latvia

<sup>3</sup> Department of Physics and Methods of Teaching Physics, Berdyansk State Pedagogical University, Ukraine

<sup>4</sup> Department of the Semiconductor Electronics Lviv Polytechnic National University, 12, Bandery st., 79046 Lviv, Ukraine

(Received 21 August 2023; revised manuscript received 17 October 2023; published online 30 October 2023)

This study investigated the optical absorption and mechanical behavior of Gd<sub>3</sub>Ga<sub>5</sub>O<sub>12</sub> (GGG) single crystals exposed to fast 84 Kr ions at fluences ranging from 10<sup>13</sup> to 10<sup>14</sup> ion/cm<sup>2</sup>. We observed that the optical absorption spectra of GGGs grown using the Czochralski method feature distinct narrow lines in the UV spectrum, attributable to the 4f-4f transitions in Gd<sup>3+</sup>. Clear changes were identified from the 6S 7/2 base state to the <sup>6</sup>P, <sup>6</sup>J, and <sup>6</sup>D states within the Gd<sup>3+</sup> cation. An unexpected absorption band was also detected at 350 nm, likely resulting from unintentional Ca contamination. After ion exposure, the fundamental absorption edge shifted by approximately 30 nm towards the longer-wavelength section of the spectrum. Our hardness tests indicated a softening effect post-ion exposure, possibly linked to ion-triggered amorphization.

**Keywords:** Gd<sub>3</sub>Ga<sub>5</sub>O<sub>12</sub> (GGG) single crystal, Swift heavy ion, Radiation damage, Amorphization.

DOI: [10.21272/jnep.15\(5\).05020](https://doi.org/10.21272/jnep.15(5).05020)

PACS numbers: 61.80.Jh, 81.05.Dz

### 1. INTRODUCTION

Gadolinium gallium garnets (Gd<sub>3</sub>Ga<sub>5</sub>O<sub>12</sub> or GGG) are versatile and find their place in applications like solid-state lasers, phosphors, and scintillators [1, 2]. GGG is a foundational lattice for luminescent materials, especially when combined with luminescent transition metals and trivalent lanthanide ions [3-5]. Characteristically, GGG single crystals are renowned for their transparency across a broad spectral range, high refractive index, and chemical stability. Moreover, they possess notable hardness and adaptability to doping with diverse impurities. Numerous studies employing ellipsometry, transmission spectra analysis, photoluminescence, and neutron diffraction have delved into their optical, thermo-optical, magnetic, and magneto-optical properties [6-8].

GGG is a garnet crystal structure family member characterized by its cubic unit cell and the space group Ia 3d [9, 10]. Recently, the focus has shifted to exploring the optical attributes and the structural irregularities in GGG single crystals, which may be attributed to the growth processes or radiation-induced defects [11, 12]. Despite a wealth of information on oxide materials like MgO, CaO, Al<sub>2</sub>O<sub>3</sub>, CdTeO and MgAl<sub>2</sub>O<sub>4</sub> [13-20], the comprehensive understanding of radiation defects and associated processes in GGG remains limited.

This limitation is primarily rooted in the absence of experimental data. This scarcity is compounded by the low proclivity of point defect formation in GGG single crystals [21]. A salient point is the yet unmeasured displacement energy (Ed) for Gd, Ca, and O in GGG, even as known values of Ed for oxygen in binary and other complex oxides hover between 50 – 70 eV [22]. To bridge this knowledge gap, we undertook a comparative evaluation of optical absorption spectra and hardness in GGG crystals posts their irradiation with 84 Kr<sup>+15</sup> ions at 1.75 MeV/nucleon for several fluences (1 × 10<sup>13</sup>, 5 × 10<sup>13</sup>, 1 × 10<sup>14</sup> ion/cm<sup>2</sup>).

### 2. EXPERIMENTAL

Gd<sub>3</sub>Ga<sub>5</sub>O<sub>12</sub> single crystals were grown using the Czochralski technique in a mildly oxidizing environment (98 % Ar and 2 % O<sub>2</sub>) at the SRC “Electron-Cfrat” in Lviv, Ukraine. The fabricated samples were shaped into flat plates, each having a 0.48 mm thickness, and were oriented along the (111) plane. Both surfaces of these plates were polished for clarity. The samples underwent irradiation by 84 Kr ions with energies peaking at 1.75 MeV/nucleon for fluences reaching 1 × 10<sup>13</sup>, 5 × 10<sup>13</sup>, and 1 × 10<sup>14</sup> ion/cm<sup>2</sup>. The ion beam's current fluctuated between 400 and 480 nA. The samples exhibited no discernible damage after exposure to these high-energy krypton ions. The irradiation procedure was executed at the DC-60 heavy ion accelerator based in Astana, Kazakhstan. To compute the ion distances and their energy dissipation within the crystal, we employed the SRIM-2013 software.

An Agilent Cary 7000 spectrophotometer was utilized for the optical absorption spectra readings. These measurements were conducted at ambient temperature, covering a spectral range from 200 nm to 1100 nm, and maintaining a resolution of 1.0 nm.

The micro- and nanomechanical attributes were assessed using the Agilent Nano G200 indentation system, a product of the USA. This system is equipped to perform the standard CSM (Continuous Stiffness Measurement) measurements, where there's a consistent recording of the exerted force and the indenter tip's displacement. These assessments were executed on the irradiated surface and surface profiles. The latter was obtained by cleaving the irradiated samples along the ion beam trajectory. Observations made on these surface profiles prove more elucidative, yielding insights into structural and mechanical changes throughout the entire span of the ion's journey. This also unveils the depth-dependent nuances, gauged as the distance from the irradiated surface. During CSM mode assessments, calibration was accomplished using bespoke samples

and methodologies provided by the instrument's manufacturer. Typically, each point underwent ten measurements, and their average value was documented.

### 3. RESULTS AND DISCUSSION

Fig. 1 shows the absorption spectrum of the  $\text{Gd}_3\text{Ga}_5\text{O}_{12}$  garnet observed at ambient temperature between 200 – 450 nm, prior to and following irradiation by swift krypton ions. The absorption pattern of a pristine GGG single crystal reveals a sequence of slender bands within the UV spectrum, which correlate with the electronic transitions in the  $\text{Gd}^{3+}$  ion.

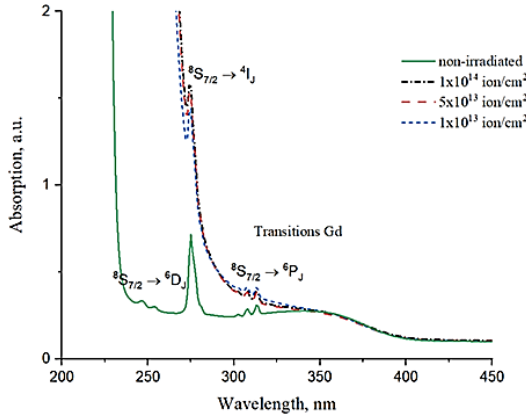


**Fig. 1** – Absorption spectrum of  $\text{Gd}_3\text{Ga}_5\text{O}_{12}$  single crystal irradiated with 147 MeV 84 Kr ions depending on the fluence

Owing to its half-filled configuration ( $f7$ ), the  $\text{Gd}^{3+}$  ion possesses a null orbital angular momentum ( $L = 0$ ). As a result, all the gadolinium ion transitions occur in the ultraviolet domain, surpassing  $32000 \text{ cm}^{-1}$ . These transitions originate from the basal state  $^8\text{S}_{7/2}$  and lead to excited states that undergo splitting by the crystal field's multiplets for the terms  $^6\text{P}$ ,  $^6\text{I}$ , and  $^6\text{D}$ . Absorption bands discernible at wavelengths 254 nm, 275 nm, and 313 nm can be respectively attributed to the transitions  $^8\text{S}_{7/2} \rightarrow ^6\text{D}_j$ ,  $^8\text{S}_{7/2} \rightarrow ^6\text{I}_j$ , and  $^8\text{S}_{7/2} \rightarrow ^6\text{P}_j$  [23]. Notably, GGG single crystals are transparent across the visible to near-infrared spectrum range. When a GGG crystal incorporates a Ca ion impurity, an auxiliary absorption band emerges at 350 nm. Preliminary analyses suggest this to be a result of oxygen vacancies linked to the Ca impurity. This spectral construct is also identifiable in GGG single crystals post-irradiation.

In irradiated single crystals, the fundamental absorption edge shift by  $\sim 30 \text{ nm}$  to the long-wavelength part of the spectrum is observed. With an increase in the fluence, the shift continues to increase, but only slightly. The observed changes are caused by structural disturbances caused by the depletion of the surface layer and an increase in the number of displaced atoms

Ion-induced deformations and distortions affect the hardness of the material by measuring the dependence of nanohardness in-depth, and, depending on the fluence, it is possible to judge the ongoing changes in the structure [24]. The measurements of hardness show ion-induced softening (Fig. 2 and Fig. 3), which can be related to ion-induced amorphization. Comparison of the depth behavior of hardness and calculated energy loss leads to the conclusion that ion-induced modifications of

structure and hardness are ensured by electronic energy loss. The threshold energy loss from data Fig. 2 is about 6 – 7 keV/nm. The effect at given fluences reaches a plateau at  $\Delta H/H_0$  of about 65 % (Fig. 3). The measurements show that the softening zone's width approaches the irradiated zone's thickness.

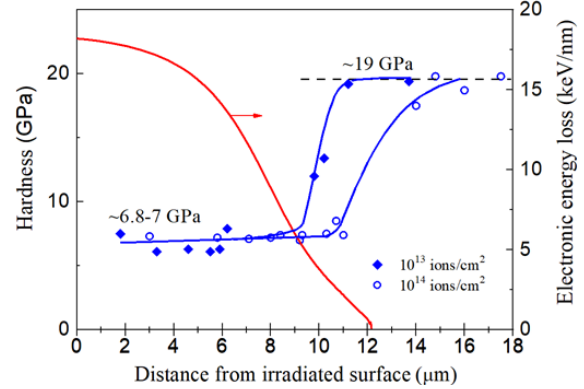


**Fig. 2** – Variation of hardness and electronic energy loss along ion trajectory on cleaved profile surface of GGG crystal irradiated with 150 MeV Kr ions at fluences  $10^{13}$  and  $10^{14} \text{ ion/cm}^2$

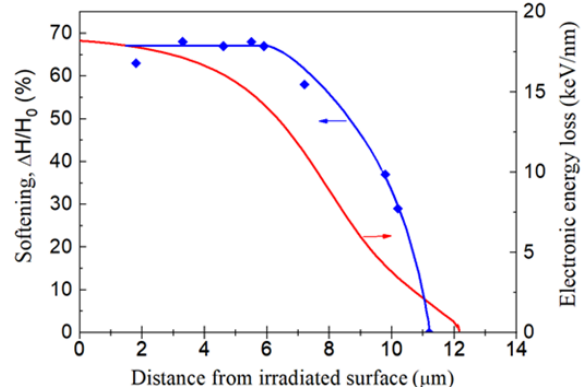


**Fig. 3** – Variation of ion-induced softening and energy loss for sample irradiated with  $10^{13} \text{ ion/cm}^2$

The behavior of a material under mechanical deformation, such as indentation, can reveal a wealth of information about its underlying microstructure, particularly differences between amorphous and crystalline states. The irradiated sample exhibits characteristics highly indicative of amorphous materials, displaying unique deformation patterns, as shown in Fig. 4.

In crystalline materials, the deformation usually occurs along well-defined planes due to the organized arrangement of atoms, leading to dislocation glide or slip along specific crystallographic orientations. However, the deformation area surrounding the indents on the irradiated sample tells a different story. Here, the shape of the deformation zone is directly contingent upon the geometry of the indenter used. Whether the indenter is pyramidal, conical, or any other form, the material deforms in a way that mirrors that geometry. This is a hallmark of amorphous materials, where the lack of long-range order in the atomic structure allows for a more uniform, non-directional deformation.

In crystalline materials, the deformation usually occurs along well-defined planes due to the organized arrangement of atoms, leading to dislocation glide or

slip along specific crystallographic orientations. However, the deformation area surrounding the indents on the irradiated sample tells a different story. Here, the shape of the deformation zone is directly contingent upon the geometry of the indenter used. Whether the indenter is pyramidal, conical, or any other form, the material deforms in a way that mirrors that geometry. This is a hallmark of amorphous materials, where the lack of long-range order in the atomic structure allows for a more uniform, non-directional deformation.

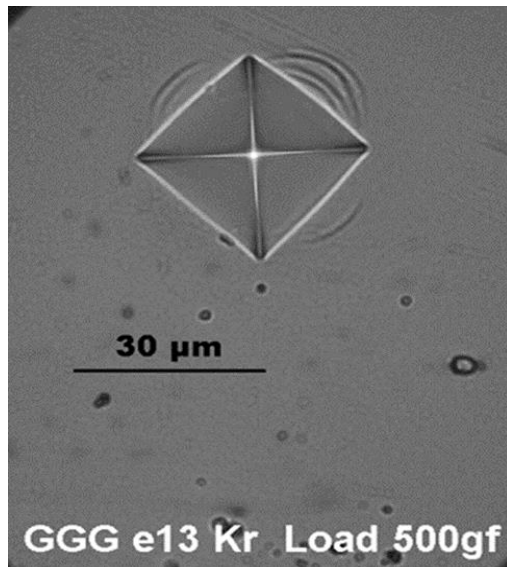


**Fig. 4** – View of deformation zone around indents on ion irradiated GGG

Another intriguing aspect is the stress distribution surrounding the indents. In amorphous materials like the irradiated sample, stress concentrates in specific regions known as shear bands. These bands are localized zones where the material undergoes severe deformation, allowing the structure to accommodate the applied force. In the sample context, these shear bands are opposite to the centers of the indenter faces. At these locations, the shear stress reaches its maximum, or zenith, suggesting that the material is undergoing high levels of plastic deformation, specifically in these regions.

Post-irradiation behavior of the material shows remarkable changes in mechanical properties, especially in terms of plasticity. The ability of a material to deform under stress without breaking is a measure of its malleability. Enhanced plasticity means the material can withstand more deformation, making it more resilient under mechanical load.

## REFERENCES

1. Q.C. Liu, X.M. Zhou, S.N. Luo, *J. Appl. Phys.* **121**, 14 (2017).
2. C. Li, Y. Wu, X. Li, L. Ma, F. Zhang, H. Huang, *J. Mater. Process. Technol.* **279**, 116577 (2020).
3. A. Krasnikov, A. Luचेchko, E. Mihokova, M. Nikl, I.I. Syvorotka, S. Zazubovich, Y. Zhydachevskii, *J. Lumin.* **190**, 81 (2017).
4. S. Kurosawa, A. Yamaji, V.V. Kochurikhin, M. Ivanov, J. Pejchal, R. Murakami, A. Yoshikawa, *Radiat. Meas.* **106**, 187 (2017).
5. K. Zhang, L. Tong, Y. Ma, J. Wang, Z. Xia, Y. Han, *J. Alloy. Compd.* **781**, 467 (2019).
6. Q. Xu, Y. Wang, F. Chen, W.H. Wong, Z.B. Zhang, D.L. Zhang, *J. Am. Ceram. Soc.* **102**, 6407 (2019).
7. C. Li, F. Zhang, Y. Piao, *Ceram. Int.* **45** No 12, 15015 (2019).
8. Y.L. Li, D. Zhang, M. Luo, Q.H. Yang, F. Fan, S.J. Chang, Q.Y. Wen, *Opt. Exp.* **29**, 23540 (2021).
9. S. Geller, *Z. Kristallogr. Cryst. Mater.* **125**, 1 (1967).
10. J. Dong, K. Lu, *Phys. Rev. B* **43** No 11, 8808 (1991).
11. A. Matkovskii, P. Potera, D. Sugak, L. Grigorjeva,

One of the most noteworthy observations is that the material does not exhibit cracks around the indents even when subjected to relatively high mechanical loads, such as 500 gf (gram-force). This is a substantial deviation from untreated Gadolinium Gallium Garnet (GGG) behavior. Cracks are generally the initiation points for catastrophic failure, and their absence signifies that the irradiated sample has enhanced toughness and integrity.

In summary, the irradiated material showcases a host of fascinating mechanical behaviors characteristic of amorphous structures. The deformation patterns depend on the shape of the indenter, localized shear bands bear the brunt of the stress, and the material exhibits remarkable plasticity and toughness post-irradiation. These observations could significantly affect the material's applications in various high-stress environments.

## 4. CONCLUSION

A comparative review of the optical absorption, X-ray diffraction data, and mechanical attributes along the ion trail for Gd<sub>3</sub>Ga<sub>5</sub>O<sub>12</sub> (GGG) single crystals subjected to swift 84 Kr ion irradiation up to fluences of 10<sup>13</sup>–10<sup>14</sup> ion/cm<sup>2</sup> reveals a noteworthy shift in the primary absorption edge-around 30 nm towards the spectrum's longer-wavelength end. This phenomenon can be ascribed to structural disruptions triggered by thinning of the surface layer and a surge in displaced atoms, predominantly oxygen. This upheaval is paired with an expansion in the crystal lattice parameter, a claim substantiated by variations in nano-hardness across the ion route. The hardness evaluations distinctly pinpoint a softening effect due to ions, potentially attributable to ion-induced amorphization.

## ACKNOWLEDGEMENTS

This research has been funded by the Science Committee of the Ministry of Science and Higher Education of the Republic of Kazakhstan (Grant No. AP14870696). In addition, the research of A.P. and Y.S. was partly supported by COST Action CA20129 “Multiscale Irradiation and Chemistry Driven Processes and Related Technologies” (MultiChem). A.P. thanks to the Institute of Solid-State Physics, University of Latvia. ISSP UL as the Center of Excellence is supported through the Framework Program for European universities, Union Horizon 2020, H2020-WIDESPREAD-01–2016–2017-TeamingPhase2, under Grant Agreement No. 739508, CAMART2 project.

- D. Millers, V. Pankratov, A. Suchocki, *Cryst. Res. Technol.* **39**, 788 (2004).
12. N. Mironova-Ulmane, A.I. Popov, A. Antuzevics, G. Kriekle, E. Elsts, E. Vasil'chenko, A. Sarakovskis, *Nucl. Instrum. Meth. Phys. Res. Sect. B* **480**, 22 (2020).
13. E.A. Kotomin, M.M. Kuklja, R.I. Eglitis, A.I. Popov, *Mater. Sci. Eng. B*, **37** No 1-3, 212 (1996).
14. E.A. Kotomin, V. Kuzovkov, A.I. Popov, J. Maier, R. Vila, *J. Phys. Chem. A* **122** No 1, 28 (2018).
15. Y. Suchikova, S. Kovachov, I. Bohdanov, V. Pankratov, A.I. Popov, *Appl. Phys. A: Mater. Sci. Process.* **129** No 7, 499 (2023).
16. D.V. Ananchenko, S.V. Nikiforov, V.N. Kuzovkov, A.I. Popov, G.R. Ramazanova, R.I. Batalov, R.M. Bayazitov, H.A. Novikov, *Nucl. Instr. Meth. Phys. Res. B* **466**, 1 (2020).
17. G. Baubekova, A. Akilbekov, E. Feldbach, R. Grants, I. Manika, A.I. Popov, A. Lushchik, *Nucl. Instrum. Meth. Phys. Res., Sect. B* **463**, 50 (2020).
18. Y. Suchikova, S. Kovachov, I. Bohdanov, A. Moskina, A.I. Popov, *Coatings* **13** No 3, 639 (2023).
19. A. Usseinov, Z. Koishybayeva, A. Platonenko, A.I. Popov, *Latv. J. Phys. Tech. Sci.* **58** No 2, 3 (2021).
20. S.O. Vambol, I.T. Bohdanov, V.V. Vambol, T.P. Nestorenko, S.V. Onyschenko, *J. Nano-Electron. Phys.* **9** No 6, 06016 (2017).
21. Z.T. Karipbayev, K. Kumarbekov, I. Manika, Y. Suchikova, A.I. Popov, *phys. status solidi b* **259** No 8, 2100415 (2022).
22. A.I. Popov, E.A. Kotomin, J. Maier, *Nucl. Instrum. Meth. Phys. Res., Sect. B* **268** No 19, 3084 (2010).
23. N. Mironova-Ulmane, I. Sildos, E. Vasil'chenko, G. Chikvaidze, V. Skvortsova, A. Kareiva, A.I. Popov, *Nucl. Instrum. Meth. Phys. Res., Sect. B* **435**, 306 (2018).
24. A. Dautlebekova, V. Skuratov, N. Kirilkin, I. Manika, J. Maniks, R. Zabels, A. Seitbayev, *Surf. Coat. Technol.* **355**, 16 (2018).

### Мікромеханічні властивості кристалів $Gd_3Ga_5O_{12}$ , опроміненних швидкими важкими іонами

G.M. Aralbayeva<sup>1</sup>, I. Manika<sup>2</sup>, Zh. Karipbayev<sup>1</sup>, Y. Suchikova<sup>3,\*</sup>, S. Kovachov<sup>3</sup>, D. Sugak<sup>4</sup>, A.I. Popov<sup>2</sup>

<sup>1</sup> Faculty of Physics and Technical Sciences, L.N. Gumilyov Eurasian National University, 010008 Astana, Kazakhstan

<sup>2</sup> Institute of Solid State Physics, University of Latvia, 8, Kengaraga, LV-1063 Riga, Latvia

<sup>3</sup> Department of Physics and Methods of Teaching Physics, Berdyansk State Pedagogical University, Ukraine

<sup>4</sup> Department of the Semiconductor Electronics Lviv Polytechnic National University, 12, Bandery st., 79046 Lviv, Ukraine

У даній статті наведені результати досліджень оптичного поглинання та механічної поведінки монокристалів  $Gd_3Ga_5O_{12}$  (GGG), підданих дії швидких іонів 84 Kr при флюенсах від 1013 до 1014 іон/см<sup>2</sup>. Установлено, що спектри оптичного поглинання GGG, вирощених за допомогою методу Чохральського, мають чіткі вузькі лінії в УФ-спектрі, що можна віднести до переходів 4f-4f у  $Gd^{3+}$ . Було виявлено чіткі зміни від базового стану 6S 7/2 до станів 6P, 6J і 6D в катіоні  $Gd^{3+}$ . Неочікувана смуга поглинання також була виявлена при 350 нм, ймовірно, в результаті ненавмисного забруднення Са. Після впливу іонів край основного поглинання зміщується приблизно на 30 нм у бік більш довгохвильової ділянки спектру. Тести на твердість показали ефект пом'якшення після впливу іонів, пов'язаний з аморфізацією матеріалу.

**Ключові слова:** Монокристал  $Gd_3Ga_5O_{12}$  (GGG), Швидкий важкий іон, Радіаційне пошкодження, Аморфізація.